

Desalination of Complex Multi-Ionic Solutions by Reverse Osmosis at Different pH Values, Temperatures, and Compositions

Marko Pranić, Edward M. Kimani,* P. M. Biesheuvel, and Slawomir Porada

Cite This: *ACS Omega* 2021, 6, 19946–19955

Read Online

ACCESS |



Metrics & More



Article Recommendations



Supporting Information

ABSTRACT: For a thorough mechanistic understanding of reverse osmosis (RO), data on ion retention obtained by desalination of multi-ionic solutions are needed. In this paper, we show how to obtain such data under controlled laboratory conditions at any nonextreme pH. For that, we propose a simple method where we use N_2 and CO_2 gas control to set the composition of a gas phase in equilibrium with the feedwater solution. By increasing the CO_2 partial pressure, the pH of the solution will decrease and vice versa. We applied this method of CO_2 gas control to extend and validate an existing data set on ion retention of multi-ionic brackish water with 10 different ionic species, whereas conditions in the prior data set were slightly uncontrolled; in our new analysis, we performed experiments at precisely controlled pH and temperature. We run experiments at pH 6.73 and pH 7.11 and in a temperature range of $T = 15–31$ °C. Our results show that when pH is decreased, or temperature increased, the ion retention of most ions decreases. We also tested the influence of the Na^+ to Ca^{2+} concentration ratio in this multi-ionic solution on ion retention at pH 6.73 and $T \sim 31$ °C. We noticed that this ratio has a larger effect on ion retention for cations than for anions. We compare our data with the earlier reported data and describe similarities and differences. The improved data set will be an important tool for future development of accurate and validated RO ion transport models. Such RO models that describe desalination performance in detail are important for successful commercial application of the RO technology. We also discuss a relevant preparation method for water slightly oversaturated with barely soluble $CaCO_3$ by solution preparation at high CO_2 pressure, after which the solution is brought to the required pH by the N_2 and CO_2 gas control method.

Parameter	Ion retention
Temp. ↑	All ions ↓
pH ↓	Na^+ , K^+ , HCO_3^- , Ca^{2+} , Mg^{2+} ↓
	NH_4^+ ↑
$\frac{Na^+}{Ca^{2+}}$ ↓	Cations ↓
	Anions ~const.

1. INTRODUCTION

Each person has the right to clean water.¹ However, nonsustainable use of water sources, industrialization, and population growth put increasing pressure on available water, leading to the current situation where many people lack enough water to meet their basic needs.² One possible solution to help solve this problem is the treatment of water sources such as seawater, brackish water, and wastewater to obtain usable water for agriculture, industry, and personal use. These sources are multi-ionic solutions, and they often contain high concentrations of salts, which hinders their direct use. Different technologies for salt removal are available to reduce the concentrations of salts to an acceptable level.³ The most developed desalination technology is reverse osmosis (RO), which is a pressure-driven membrane separation process.⁴ Today, ~70% of all water produced by desalination comes from RO desalination plants,⁵ and in the coming years, the global capacity of water produced by RO is expected to increase.⁶

The key to having a cost-efficient and energy-efficient RO desalination plant is to be able to predict process performance in detail, and for that, RO simulation software is used. With that software available, optimal conditions for running an RO installation can be determined, quality of permeate and retentate water can be estimated, and process optimization

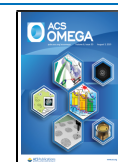
can be more direct.⁷ Software for a full RO installation plant includes an RO ion transport model as a key part. These models are also relevant in the design of new membranes with improved characteristics and desalination performance.^{8,9}

When we develop improved mechanistic RO ion transport models, two things are required. First of all, a good understanding of the physical and chemical phenomena responsible for ion transport and a mathematical model are needed. Second, to accurately estimate the model parameters and validate the model predictions, reliable experimental data under relevant conditions are required. In this paper, we focus on this second aspect, on how to obtain high-quality data of water desalination with an RO membrane, for a certain multi-ionic solution. We provide significant emphasis on the methods that enable us to obtain and maintain desired pH values.

Received: June 4, 2021

Accepted: July 9, 2021

Published: July 21, 2021



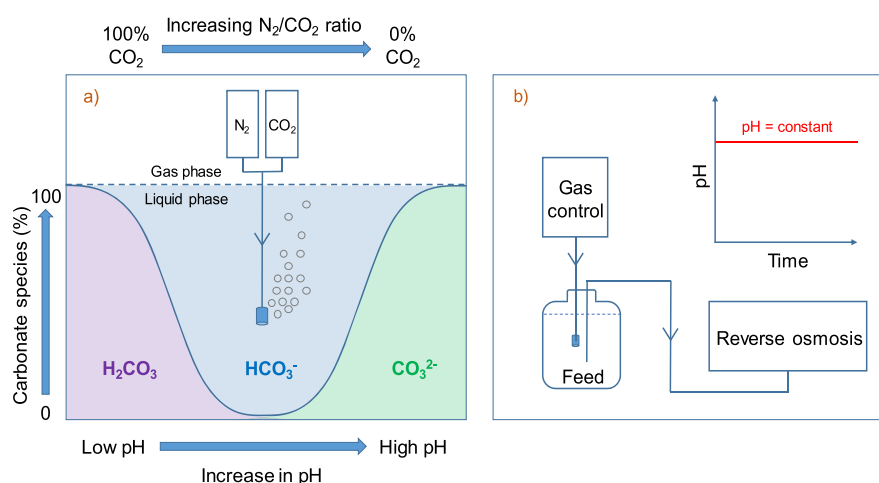


Figure 1. Schematic summary of the presented methodology. (a) Novel developed gas control method to vary pH of a multi-ionic aqueous system by manipulating carbonate chemistry. (b) Application of the method to the case of RO to obtain data with precisely set pH values of the feedwater.

We present experimental data on ion passage obtained by desalination of multi-ionic solutions with 10 different ionic species for laboratory conditions. Ion passage, P , is defined as the percentage of the ions that passes through the membrane and is given by $P = c_{\text{perm}}/c_{\text{feed}}$, typically expressed as a percentage. Here, c_{feed} and c_{perm} are the concentrations in the feedwater and in the permeate. A similar term is ion retention, R , which is given by $R = 1 - P$, again typically expressed as a percentage. We also report the conditions that influence ion passage, most importantly, feedwater pH, temperature, and certain hydrodynamic factors such as the water flow rate.

The novelty of the laboratory RO setup that we use, compared to other setups reported in the literature, is the use of precise N_2/CO_2 gas control, as shown in Figure 1. This gas control method enables us to set and maintain constant feedwater pH during the full duration of RO experiments by adjusting the N_2/CO_2 ratio of the gas bubbled through the feedwater (which in our case is a multi-ionic solution). Gas control also removes excess CO_2 , which was an important step during solution preparation to lower water pH and dissolve sparsely soluble CaCO_3 . This method also removes dissolved O_2 from water, thereby more closely replicating the anaerobic conditions present in anaerobic groundwater. This is important because, if possible, anaerobic conditions should be maintained in desalination plants to reduce the feedwater redox potential, and consequently, reduce the risk of scaling.¹⁰

The multi-ionic solution that we use is of significant interest because it is an example of the natural groundwater used in a water treatment plant. This solution also contains amphoteric ammonium and carbonate ions, which can react both as an acid and base, and thus can be present in two different ionic states at the same time in solution.¹¹ Acid–base equilibrium is known to influence RO operation,^{12,13} and because of that, our data are valuable for the development of RO transport models that include this equilibrium. Our data set is furthermore of importance because reported RO experiments for laboratory conditions are generally not done with multi-ionic solution as feedwater. However, most lab-based data on ion passage in RO were obtained from simple solutions with just a few ionic species. However, the effects that are present in simple solutions are not necessarily the same as in multi-ionic solutions.¹⁴ Instead, when data of multi-ionic solutions are reported in the literature, it is often not based on laboratory

conditions, but from actual operation of desalination plants, and that has several implications. It often means that data are not readily reproducible, there is no good control over the ion composition of feedwater, desired experimental conditions are not easily obtained. These are significant drawbacks of data sets obtained in field conditions. Our approach is thereof of relevance, namely, we obtained data for multi-ionic solutions under controlled laboratory conditions. Therefore, data are reproducible, more operational conditions are possible, and the data set can at any (later) time easily be extended with more experimental conditions.

We prepared a multi-ionic solution according to the ion composition of anaerobic groundwater reported by Biesheuvel et al. (2020) based on a groundwater source from near the city of Woerden in The Netherlands. In the same paper, data on ion passage were obtained by desalination of this water source with a membrane module operating on the site of the water treatment plant. In the present paper, we replicate these data under laboratory conditions using a dedicated RO membrane filtration unit that included a membrane cell (details below in Section 2.3). To replicate fairly, it is of importance to have the same transmembrane water flux (TMF), which is one of the key parameters influencing ion passage.¹⁵ We also made sure that the experiments were done at a similar crossflow velocity (water velocity along the membrane). This flow rate is also of importance because the value thereof influences how far the feedwater is concentrated and thus determines the risk of scaling and concentration polarization.¹⁶ Details of the experimental conditions can be found in Table S1 in the Supporting Information, which shows a detailed comparison of the present experimental conditions, and those reported by Biesheuvel et al. (2020) for the onsite data. In our laboratory program, we obtained data for ion passage for all ions at two different pH values (pH 6.73 and pH 7.11) and for various values of temperature in the range of $T = 15\text{--}31$ °C. Besides that, just as in the study by Biesheuvel et al. (2020), we measured ion passage for three differently modified, or “spiked”, compositions where the Na^+ -to- Ca^{2+} concentration ratio (CCR for “cation concentration ratio”) of the solutions was changed. This is an important parameter because the ratio of the concentration of monovalent ions to divalent ions in solution is known to influence RO membrane ion passage, and

Table 1. Standard Ion Composition of Natural Brackish Groundwater Used as a Multi-Ionic Solution in RO Experiments^a

ion	Na ⁺	K ⁺	NH ₄ ⁺	Ca ²⁺	Mg ²⁺	Cl ⁻	HCO ₃ ⁻	SO ₄ ²⁻
<i>c</i> (mM)	2.50	0.137	0.164	2.90	0.656	2.70	6.43	0.386
<i>c</i> (mg/L)	57.4	5.36	2.96	116	15.9	95.4	392	37.1

^aIon composition of the case I experiment, reported in the study by Biesheuvel et al. (2020). Cases II–IV are shown in Table S2.

this effect should be predicted accurately by RO ion transport models.¹⁷

In the study by Biesheuvel et al. (2020), such data on ion passage were used to develop the ion transport model based on the extended Donnan steric partitioning pore model (ext-DSP model), a model which includes acid–base equilibria of all ions. The new data in this paper can be used to further develop that line of modeling or other RO transport models.

2. MATERIALS AND METHODS

2.1. Multi-Ionic Solutions. The feedwater for our RO experiments was a multi-ionic solution prepared to be similar to the water obtained from a pumping station located 1.5 km north-west from the city of Woerden in The Netherlands. This anaerobic groundwater was pumped from a sandy layer 15 to 40 m deep, above which is a layer of peat, which is the source of relatively large concentrations of NH₄⁺ in this water. The ion composition of groundwater can be found in Table 1. Preparation of this solution in the laboratory was difficult because a high amount of sparsely soluble CaCO₃ salt has to be dissolved. However, we successfully prepared the solution using CO₂ bubbling to decrease pH and dissolve CaCO₃, after which we removed excess CO₂ with N₂/CO₂ bubbling. For details on this preparation method, see section 3 in the Supporting Information.

In the study by Biesheuvel et al. (2020), this water is called brackish groundwater. However, its salinity (TDS ~ 722 mg/L) is very low for brackish water, and some sources would describe it as fresh groundwater. Because it has a high mineral content of more than 180 mg/L CaCO₃, it would fall under the classification of very hard freshwater.¹⁸ Also, according to an EU directive, it can be considered as mineral water with intermediate mineral concentration (TDS = 500–15000 mg/L).¹⁹ In this paper, we call it multi-ionic solution. We also use the term case I when discussing an experiment with this multi-ionic solution (of which the composition is given in Table 1) without adding any extra salts. We also discuss cases II, III, and IV for experiments in which we added salts to the multi-ionic solution (of the composition provided in Table 1) to achieve different CCR in the feedwater. A discussion on how to prepare each solution can be found in the Supporting Information. In all these cases, the feedwater meets all safety requirements for human consumption, except for the high level of NH₄⁺ of 3 mg/L. EU legislation sets the limit for the NH₄⁺ concentration in drinking water at 0.5 mg/L.²⁰ Besides NH₄⁺, one other amphoteric ion in this solution is bicarbonate, HCO₃⁻, and the related species carbonic acid and the divalent carbonate cation. Their presence makes this solution interesting for theories and models that include acid–base equilibria.

Visual MINTEQ, a chemical modeling software, can be used successfully for the theoretical analysis of aqueous solutions.^{21,22} In this work, this software was used for three purposes, first to predict the likely pH of multi-ionic solutions at different gas compositions, second, to evaluate under which conditions there is a risk for precipitation, and third, to

determine which species are predicted to be present for each pH and temperature.

2.2. Method for pH Control by Manipulating the Carbonate Chemistry. In this paper, precise pH values were attained in a feedwater solution by adjusting the partial pressure of CO₂ in a gas phase in equilibrium with the feedwater. At a certain partial pressure of CO₂, there is a related concentration of CO₂ in water according to Henry's law.²³ Dissolved CO₂ can form different carbonate species. They are carbonic acid (H₂CO₃), bicarbonate (HCO₃⁻), and carbonate (CO₃²⁻) ions. The partial pressure of CO₂ will influence the concentrations of these species and, consequently, will influence pH.²⁴ We used this phenomenon as the basis of our method. To illustrate, it is useful to analyze two extreme scenarios. The first extreme is when the CO₂ partial pressure is 100% (mol %), which can be achieved with pure CO₂ gas bubbling. As a result, CO₂ will react with water to create H₂CO₃, which decreases pH. The second extreme is when a solution is bubbled with N₂, and the partial pressure of CO₂ is zero. Now, pH will increase, and the distribution among the carbonate species will shift toward HCO₃⁻ and CO₃²⁻. In our method, we combine N₂ and CO₂ bubbling into one method, in which we can vary the inflow ratio of these gases, and as a consequence, we can accurately change the CO₂ partial pressure. And, in this way, it is possible to obtain any pH in solution in between these two mentioned extreme situations. We call our method N₂/CO₂ gas control, and it is graphically illustrated in Figure 1.

The N₂/CO₂ gas control apparatus is easy to construct from readily available laboratory equipment. It consists of tubing and two mass flow meters (Mass-View, Bronkhorst, The Netherlands), one for each gas. The flow meters for N₂ and CO₂ are placed between pressurized gas sources and a connection point, or mixing point, where the two separate gas streams are mixed by joining the separate tubes for each gas into one tube. At the end of this common tube that transports the N₂/CO₂ mixture, there is a gas dispenser (for instance, a sparging device) that is inserted into water. When the gases start to flow, the feedwater is bubbled through and the gas composition in equilibrium with the solution is changed. By increasing the N₂ flow or decreasing the CO₂ flow, relative to one another, pH increases and vice-versa. Thus, by tuning the settings of the flow meters, we can easily set the flow of each gas to achieve the desired pH. Note that the exact values of the two flows are not decisive in this type of experiment. Instead, what controls pH is the ratio between the concentrations of N₂ and CO₂ in the gas flow, that is, the gas composition. The same ratio and composition can be achieved at different gas flows. For the multi-ionic solution described in this paper, this ratio was around 10/1 for pH 6.73 to 30/1 for pH 7.11, with the larger flow rate that of N₂. To achieve the constant pH, bubbling was continued during the entire experiment, and the solution was open to the atmosphere, so that the total pressure remained constant.

2.3. RO Experiments. RO experiments were performed using a cross-flow lab-scale membrane filtration system

(Convergence Inspector Colossus, Convergence, The Netherlands) connected to a homemade stainless steel membrane cell. The temperature in the system was maintained with a cooling system. A detailed description of the equipment and a flowchart of the setup can be found in [Supporting Information](#). In the experimental work, two different pieces of membrane (membrane A and B) of a low-pressure thin-film composite RO membrane (ESPA2-LD-4040, Hydranautics, USA) were used (area 250 cm²). The pieces were obtained from membrane sheets by cutting open a RO membrane module. Each membrane piece was placed in a membrane cell together with a feed flow spacer cut from the same membrane module as the membrane. The membrane was then hydrated for 12 h by running the RO setup with demineralized water without applying a pressure. Finally, the membrane was pressurized at 15 bar for 6 h, again with demineralized water, and after that immediately used for the experiments.

2.3.1. Experimental Conditions and Procedure. All data on ion passage presented in this paper were obtained at a T_{MF} of 20.3 LMH (LMH for L/m²/h). To achieve this T_{MF}, with the area of 250 cm², the permeate flow was 0.507 L/h. This flow was maintained by controlling the retentate pressure with a control valve; see the setup flowchart in the [Supporting Information](#). The feed flow rate was kept constant at 30 L/h, which means that only 1.67% of water goes through the membrane (water recovery = 1.67%). All experiments were done with full recirculation of permeate and retentate back to the 20 L feed tank.

We performed two types of experiments, and each lasted for 4 days. First, we ran the RO setup with membrane A, for cases I–IV (which have a different CCR), the same as reported in the study by Biesheuvel et al. (2020). For information about these cases I–IV, see [Table S2](#). Before each new experiment, we recirculated the system with a solution of similar composition for 2 h without pressure, at pH ~ 6, as a precaution to remove scaling that might have happened during the previous experiment. RO experiments are done at pH 6.73. This pH was selected because, according to Visual MINTEQ, at that pH there is no precipitation for case I, while there is precipitation at pH 7.11, which is an average value of pH reported by Biesheuvel et al. (2020) for case I. We did not decrease pH further because the aim was to replicate the earlier data, and if we would reduce pH, we would deviate even more from the original condition. However, as shown below, we discovered later that we could also run robust experiments at pH 7.11. Samples (feed and permeate) were taken after 12 h of system operation and a duplicate pair after another 1 h. For this first set of experiments, feed temperature was not controlled, and it varied between $T = 30\text{--}32$ °C. For the permeate flux of 0.507 L/h, all cases were run with a transmembrane pressure (TMP) = 11.1–11.4 bar. Results of these experiments are shown in [Figures 3](#) and [S2](#).

After all data on ion passage from experiments on different cases were obtained, this membrane A experienced a pressure spike during rinsing (the effect of pressure spikes on membrane integrity is discussed in section 2.1 in the [Supporting Information](#)). Therefore, we replaced membrane A by membrane B for a second type of experiment, in which we investigated the influence of pH and temperature on ion passage, only for case I. Results of experiments with membrane B are shown in [Figure 4](#). The experiment was started in the same way as previously, and after we took samples at pH 6.73, we changed to pH 7.11. After 2 h, under stationary conditions,

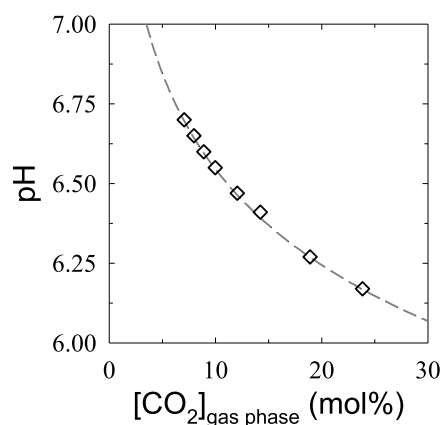


Figure 2. Dependence of solution pH (of the multi-ionic solution defined by the composition given in [Table 1](#)) on the CO₂ concentration in a gas phase in equilibrium with the solution. Diamonds are experimental data obtained with the N₂/CO₂ control method, and the line is based on theoretical equilibrium calculations (Visual MINTEQ) including a small vertical offset (see the main text).

we took a sample at this increased pH. After that, we changed conditions to pH ~ 6 to decrease the risk of precipitation, and then, we changed the temperature of the feedwater with our temperature control system. Once a new temperature set point was reached, we changed to pH 6.73. In this way, we repeated the procedure at different values of pH and temperature. We obtained data in a temperature range of $T = 15\text{--}31$ °C, and because at low temperature, the resistance to water flow is much higher; we had to vary pressure between TMP = 8.0 and 12.8 bar to obtain in all cases the same T_{MF} as in the first experiment.

2.4. Analysis. **2.4.1. Micro Gas Chromatography.** The composition of the gas phase in contact with the solution was measured with micro gas chromatography (μ -GC) with a thermal conductivity detector (Varian CP-4900 μ GC, Agilent Technologies, USA). We took one gas sample each time we collected a feedwater sample for ion composition measurements to measure the N₂/CO₂ ratio. Example results for this ratio (expressed as CO₂ mole fraction) for an experiment with pH of 6.1–6.8 can be found in [Figure 2](#). The line that fits the data is a theoretical prediction by Visual MINTEQ shifted up by 0.03 pH point.

2.4.2. Feed and Permeate Sampling. To calculate passage of each ion, the ion composition of feed and permeate must be measured. Pairs of samples were taken under stationary conditions from the feedwater and from the permeate. Samples from the feedwater were taken directly from the 20 L feed tank, and for the permeate, samples were taken right after the membrane cell by briefly diverting the permeate flow to a sample container. During each sampling, we measured pH of the feed and permeate and temperature of the feed. Samples were diluted and prepared for analysis immediately.

2.4.3. Ion Detection. Concentrations of Na⁺, K⁺, Ca²⁺, and Mg²⁺ were measured by PerkinElmer inductively coupled plasma optical emission spectrometry, type Optima 5300 DV (ICP–OES) and by Metrohm 930 compact ionic chromatography (IC) with a built-in conductivity detector. There was no significant difference in detected ion concentrations with the mentioned methods except for Ca²⁺. The reason for the difference between the measured values for the concentration

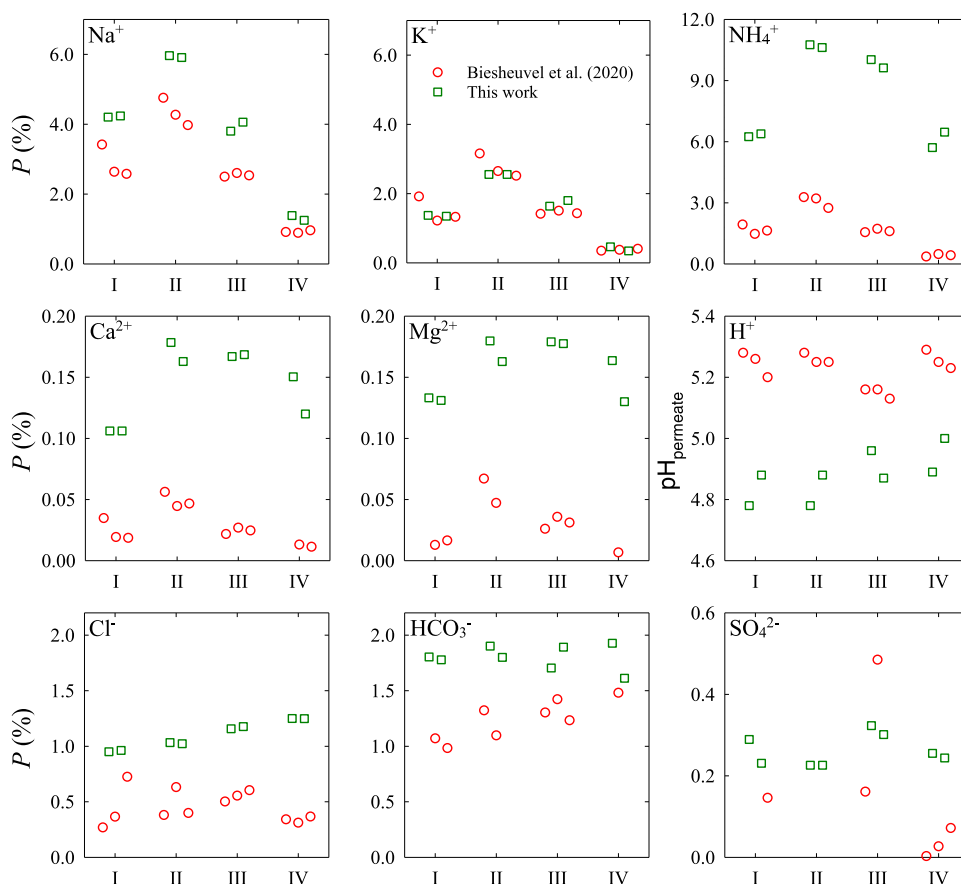


Figure 3. Data on ion passage, P , for cases I–IV with different $\text{Na}^+/\text{Ca}^{2+}$ concentration ratios (CCR) in feedwater and the permeate pH. In case I, CCR = 0.86 (ionic strength, $c_\infty \sim 14$ mM), and for cases II–IV, CCR = 0.43, 0.86, and 3.44 ($c_\infty \sim 25$ mM). Green squares represent our new data (pH 6.73, $T = 30\text{--}32$ °C, membrane A), and red circles are data obtained from the study by Biesheuvel et al. (2020) (pH 7.11, unknown temperature). Passage, P , calculated from data given in Tables S4 and S5.

of Ca^{2+} is discussed in the Supporting Information. Cation concentrations reported in the Supporting Information are from ICP–OES, except for NH_4^+ , which was only measured by IC. For anions, Cl^- and SO_4^{2-} were also measured with IC. The quality of analysis was checked with control samples and with Shewhart control charts, and in these reference experiments, the measured concentrations, presented in the Supporting Information, were within $\pm 5\%$ of the calibration values. Except for the ions mentioned above, and HCO_3^- , no other ionic species were found. We attempted to measure the concentration of HCO_3^- with different analytical techniques, but the results were always lower than what is expected based on an overall charge balance (of all ions together in solution). This may be because the CO_2 -controlled conditions in our experiments could not be maintained during sampling and analysis. Thus, during and after sampling, CO_2 could evaporate from the sample. To precisely measure HCO_3^- in the system that uses gas control in the way we describe in this paper, one would need to use a fast, reliable, and preferably in situ method for HCO_3^- detection.²⁵ Thus, to circumvent this problem, results on HCO_3^- concentration in this paper, for example, as shown in Figures 3 and 4 and Tables S4–S9, are from the charge balance method, just as was the case in the study by Biesheuvel et al. (2020).

3. RESULTS AND DISCUSSION

3.1. Potential Applications of the N_2/CO_2 Gas Control Method. An interesting question is which pH values can be obtained with the method of controlled N_2/CO_2 bubbling. This actually depends critically on the solution chemistry. For example, the range is $\sim\text{pH } 4\text{--}7$ for a NaCl solution as predicted by the Visual MINTEQ software. Removing all CO_2 indeed leads to pH 7, which was confirmed in an experiment in which NaCl solution was bubbled with N_2 . This pH value makes sense because there are no carbonate species present, and there is nothing that could result in a pH different from the neutral value of pH 7 (under standard conditions). Carbonate species can be introduced with CO_2 bubbling, and when the NaCl solution is contacted with pure CO_2 gas, pH quickly dropped to pH 4. However, if a solution is prepared by dissolving carbonate salts, similar to preparing synthetic natural water, then bubbling with N_2 will not remove all carbonate species from solution. This is probably because pH strongly increases and carbonate salts precipitate at high pH. Visual MINTEQ predicts that in equilibrium, bubbling multi-ionic solution with N_2 results in $\sim\text{pH } 12$ and contacting with pure CO_2 results in $\sim\text{pH } 5.5$. These values were not checked experimentally, but we did an experiment in the $\sim\text{pH } 6.1\text{--}6.7$ range to validate the Visual MINTEQ predictions; see the good fit shown in Figure 2. In this experiment, the N_2/CO_2 ratio was varied and pH was measured. Experimental results of the gas composition were measured by $\mu\text{-GC}$. Theoretical

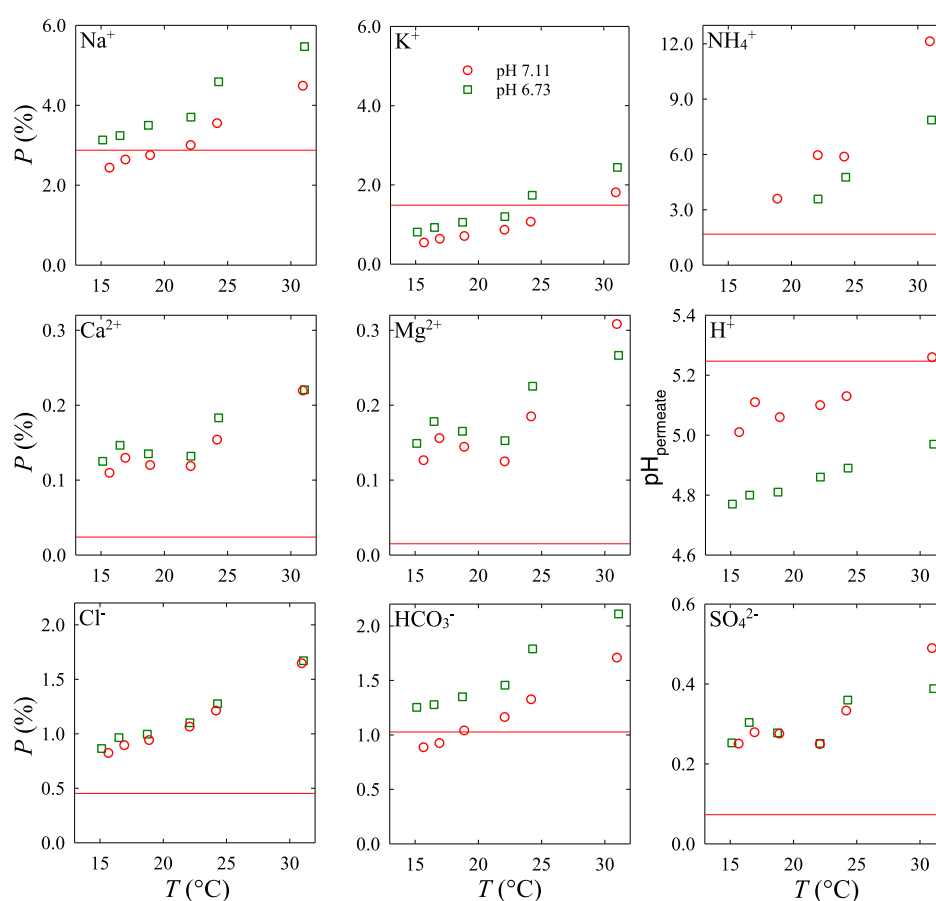


Figure 4. Data for ion passage, P , as function of temperature, T , at two different pH values (green squares are results at pH 6.73 and red circles are at pH 7.11). Data were obtained by desalination of multi-ionic solution (case I; membrane B). Horizontal red lines are average of the results reported in the study by Biesheuvel et al. (2020) with a solution of similar composition at pH 7.11 and unknown temperature. Passage, P , is calculated from data that are given in Tables S6–S9.

calculations were obtained with Visual MINTEQ, and as shown in Figure 2, these calculation results are presented as a line but shifted up by a 0.03 pH point. This is only a slight deviation, after which the theoretical line closely describes the experiments. Thus, we can conclude that Visual MINTEQ is a reliable tool to accurately predict the required partial pressure of CO_2 , that is, mole fraction of CO_2 , that is, N_2/CO_2 ratio, to establish a certain desired pH of a solution.

In our experimental program, we used the new method of N_2/CO_2 gas control to set and maintain a constant pH of synthetic brackish feedwater for RO experiments. These experiments lasted over several days, and during all this time constant, pH was easily established. This was the experiment that we investigated, but of course, our method can also more generally be used for other studies where setting a precise pH is desired. For example, a similar method was used in the study by Legrand et al. (2018) to test the ability of membrane capacitive deionization to capture CO_2 from solutions at different CO_2 partial pressures.²⁶ Also, in the study by Torres et al. (2008), different CO_2 /air mixtures were used in an experiment with a microbial fuel cell to show that carbonate species transport OH^- from a cathode to anode compartment.²⁷ Many studies report the influence of carbonate species on the degradation and fate of toxic components such as arsenic ions or organic micropollutants.^{28–31} Carbonate species are omnipresent in natural waters and will chemically interact with micropollutants, and these interactions are pH-

dependent. Our pH-adjustment method can be useful to investigate the effect of pH and carbonate concentration on the fate of micropollutants in such studies. Another aspect of the N_2/CO_2 gas control method is that we obtained the anaerobic conditions required to simulate the groundwater source. However, for other applications, when aerobic conditions are desired, O_2 or air can also be used instead of N_2 or CO_2 to control carbonate concentration and pH. Note that in experiments that use solutions with no or low buffer capacity, maintaining a precise pH can be more difficult with our method. For the experiments in this study, maintaining the precise pH was not an issue because of the high carbonate buffer capacity.

3.2. Importance of Theoretical Species in Multi-Ionic Solutions. In the study of the composition of multi-ionic solutions and ion retention in RO, it is important to realize that the “form” of the ion as it is measured is not the same as the ion speciation in solution. Indeed, Table 1 as we will explain in Section For example, Visual MINTEQ predicts that around 70–90% of the total calcium, magnesium, and sulfate, in cases I–IV, is present as unassociated divalent ions, with the remainder in the form of ion pairs. More information about ion speciation is given in the Supporting Information, which is especially important for Ca^{2+} (and the difference in its measurement by ICP and by IC), because the multi-ionic solution is close to CaCO_3 precipitation, and for some situations (cases II and III and pH 7.11), Visual MINTEQ

predicts oversaturation with CaCO_3 , increasing when pH or temperature increases.³² However, during our experiments, no precipitation or scaling of any kind was observed, nor any change in experimental conditions that could indicate precipitation. There was also no report of scaling in the related study by Biesheuvel et al. (2020).

The ion speciation effects just discussed must also be considered in the future theoretical work on developing RO ion transport models. Not only the potential effect of scaling but also the transport of ions, neutral species, and ion pairs through the RO membrane must be considered. As an example, Kimani et al.¹³ (2021) showed the importance of including the ion pairing equilibrium in the ext-DSP model.

3.3. Experiments with Multi-Ionic Solution at Different Compositions. Data of ion passage in RO for experimental cases I–IV with different $\text{Na}^+/\text{Ca}^{2+}$ concentration ratios (CCR) are shown in Figure 3. Green squares describe our new results at a feed conditions of $T = 30\text{--}32\text{ }^\circ\text{C}$ and pH 6.73. Red circles are the previous data on ion passage reported in the study by Biesheuvel et al. (2020), at unknown temperature and an average pH of pH 7.11. Both experiments were done at a $\text{TMF} = 20.3\text{ LMH}$.

Some differences and similarities can be noticed when these two data sets are compared. The most obvious difference is that in our new data, for most ions, ion passage is larger than in the previous data set. One possible reason for this difference is that our experiments were performed at different pH and temperature, which—as we will explain in Section 3.3—result in higher ion passage. To test these effects, we performed an experiment (for case I) in which we varied pH and temperature, the result of which we summarize in Figure 4. Results clearly show that pH and temperature influence ion passage. Points of similarity between the two data sets presented in Figure 3 are that the ion passage of the divalent ions is lower than that of monovalent ions, which also logically follows the Donnan exclusion theory (because divalent ions are larger and have a higher charge).³³ Also, from both data sets, it can be observed that CCR in the multi-ionic feedwater influences ion passage through the membrane. Decreasing the ratio (as in case II) increases the passage of all cations and vice-versa when CCR is increased, and the passage of all cations goes down (as in case IV). At the same time, the passage of anions does not change as much as the cations when CCR is changed. Therefore, we also conclude, as in the study by Biesheuvel et al. (2020), that the feedwater CCR influences ion transport.

In the future work, theories and ion transport models should be developed to explain the influence of CCR on ion passage. For that, both the previous and the new data sets shown in Figure 3 should be considered. The previous data set was obtained using a full membrane module, but these data are not fully satisfactory because feedwater temperature was not reported, and there were many outliers in measured concentrations, especially for SO_4^{2-} . Also, feedwater pH varied between experiments. In our new data set, all data were obtained at a controlled pH with the N_2/CO_2 gas control method, temperature was accurately measured, and we have complete and reliable measurements for the concentration of SO_4^{2-} . Note that we only tested in this experiment one membrane piece, but ideally multiple such coupons are tested, taken from the same or from different modules, as it is known that there can be up to a 20% difference in TMF for different membrane pieces, as a result of uneven manufacturing.³⁴ To

reduce this uncertainty, RO experiments can be done with multiple membrane modules that are put in series or parallel.

3.4. Experiments with Multi-Ionic Solution at Different pH values and Temperatures. In Figure 4, data on ion passage for different ions obtained by desalination of multi-ionic solution (case I) in the temperature range of $T = 15\text{--}31\text{ }^\circ\text{C}$ and at two different pH values are plotted. Selected values were for pH 6.73 and 7.11 because these are pH values of the four cases tested in this paper and in the study by Biesheuvel et al. (2020). Because one goal of this experiment was to determine if we can obtain under laboratory conditions similar ion passage for multi-ionic solution as reported in the study by Biesheuvel et al. (2020), we report in Figure 4 by a red line the ion passage at pH 7.11 from the 2020 paper. As mentioned, this work did not report temperature. However, we do know that experiments were done in the month of December (2013) at a water treatment plant near the city of Woerden in The Netherlands. The temperature of groundwater in this part of Europe is anywhere in between the range $T = 5\text{--}20\text{ }^\circ\text{C}$ for different aquifers.³⁵ Thus, likely the temperature in the experiments in the study by Biesheuvel et al. (2020) was less than in this study, where it was $T = 30\text{--}32\text{ }^\circ\text{C}$.

Our data clearly show that temperature and pH influence the ion passage. There is a gradual increase in ion passage as temperatures increase. In Figure 4, one can observe that this increase is quite similar for most ions; increasing temperature from $T = 15\text{--}31\text{ }^\circ\text{C}$ increases ion passage by around 1.5–3 times. Only for NH_4^+ , this increase is possibly larger because no NH_4^+ could be detected at lower temperatures. Temperature also affects the water passage. This can be observed in Figure 5, which shows the required increase in TMP to obtain

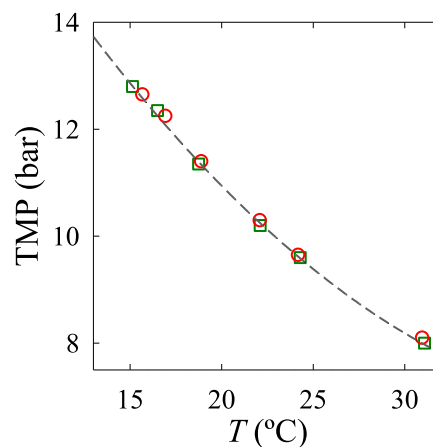


Figure 5. Required TMP, at different temperatures, T , to obtain a constant transmembrane permeate flux of $\text{TMF} = 20.3\text{ LMH}$ for results presented in Figure 4. Green squares are results at pH 6.73 and red circles at pH 7.11. The dashed line is to guide the eye.

constant TMF when temperature is decreased. For the decrease in temperature from $T = 31\text{ }^\circ\text{C}$ to $T = 15\text{ }^\circ\text{C}$, we had to increase pressure from $\text{TMP} = 8.0\text{ bar}$ to $\text{TMP} = 12.8\text{ bar}$ or else the TMF would decrease.

To understand why an increase in temperature results in a corresponding increase in ion and water passage, we can look at how temperature affects the solution and the membrane. An increase in temperature will decrease the solution viscosity, increase its osmotic pressure, and increase solute diffusivity.³⁶ Temperature also affects the solution chemistry. As shown in

section 4.1 in the Supporting Information, bicarbonate and ammonium acid–base equilibria are shifted with the temperature and pH change. Also, a higher temperature will affect the pore size and density of a membrane, and generally, the membrane becomes more permeable.³⁷ Concentration polarization is another effect that has been reported to be temperature-dependant, and as temperature increases, it is expected to decrease.³⁸ As a result of the mentioned effects, ion passage (see Figure 4) and water passage (see Figure 5) through the membrane increase at higher temperatures. A future work that use data from this paper should try to explain which of the mentioned effects of temperature are more dominant and if some can be neglected under our operating conditions. Developers of ion transport models should aim to include temperature effects in their model, thus help in understanding temperature-related phenomena.

Besides temperature, pH also influences the ion passage of multi-ionic solutions. For a small increase in pH from 6.73 to 7.11, we observed that passage of most cations decreases. In Figure 4, it can be observed that this effect was higher for Na^+ and K^+ , while for Ca^{2+} and Mg^{2+} , the effect was minor. For NH_4^+ , it is the opposite, and an increase in pH decreases NH_4^+ ion passage. For the anions, Cl^- and SO_4^{2-} change in pH did not noticeably change ion passage, and the effect for HCO_3^- was the same as for Na^+ and K^+ . Though there has been much research on the effect of pH on RO performance, we did not find a discussion on how pH influences ion passage of individual ions in multi-ionic solutions. However, our results clearly show that pH affects ion passage for most of the ions. The influence of pH on the ion passage for simple solutions was successfully modeled using an RO ion transport model that includes Donnan electrostatic exclusion in ref 40. Indeed, a model used in the study by Coronell et al. (2013) explained that as pH increases, the charge density of the active layer becomes more negative, and as a result of that, anions are better rejected. Because the electroneutrality has to be attained in the permeate,³⁹ the ion passage of the counterion is also hindered.⁴⁰ Hoang et al. (2010) showed that around neutral pH with an increase in feed pH, the membrane becomes more negatively charged, bringing about an increase in Na^+ and Cl^- rejection. They concluded that the reason for the more negative surface charge at higher pH is the deprotonation of carboxyl groups and adsorption of OH^- on the membrane.⁴¹ Van Wagner et al. (2009) also reported an increase in NaCl rejection as pH increases.⁴² In both studies with NaCl solution, it was emphasized that even though ion passage changed, pH did not significantly influence the water flux. In Figure 5, it can be observed that this was also the case in experiments in this study, that pH did not influence TMP for a certain TMF.

As shown in Figure 4, it is evident that both pH and temperature have a significant influence on the ion passage and that by increasing pH and decreasing temperature, we approached more closely the results in the study by Biesheuvel et al. (2020), see the corresponding red line, and in the case of Na^+ , K^+ , and HCO_3^- , we even obtained the same results. Another factor that influences ion passage—shown in our results—is membrane quality. Data presented in Figure 3 were obtained with membrane A and, in Figure 4, with membrane B. Because both membrane pieces are from the same membrane sheet, they should show very similar performance. However, careful analysis of Figures 3 and 4 shows that under the same conditions, ion passage is different, and membrane A has a performance that is superior to that of membrane B. For

example, at pH 6.73 and temperature $T \sim 31$ °C, ion passage of Na^+ is $\sim 30\%$ higher with membrane B. One possible explanation for this difference are the imperfections created in the membrane structure during membrane manufacturing. A higher density of such imperfections will lead to a lower performance.⁴³ Nevertheless, both membranes A and B have a very high retention of salts, allowing for the production of usable water. However, in the development of ion transport models, a difference of 30% will lead to clear differences in values of the derived membrane transport parameters. To avoid that, it is necessary to do experiments on multiple membranes to gain insights into average membrane performance.

4. CONCLUSIONS

In this paper, we described a new method of N_2/CO_2 gas control that can be used to set and maintain pH of a multi-ionic solution by adjusting the partial pressure of CO_2 in a gas phase in contact with the solution, without the need to add acid or base. Visual MINTEQ or similar software can be used to evaluate which pH values can be achieved for any type of solution, as function of gas phase composition. We used this method in a study of water desalination using RO experiments, but our method can also be considered for other experiments in which precise pH control is required.

In our RO study, using the gas control method, we obtained precise data on ion passage (or ion retention) of individual ions during the desalination of a multi-ionic solution with 10 different ionic species at precisely tuned pH values (and precisely set temperatures). We developed a data set with the aim to replicate a prior data set reported in the study by Biesheuvel et al. (2020) that specifically studied the influence of the concentration ratio between the cations Na^+ and Ca^{2+} (CCR) on ion passage. In many aspects, we obtained similar trends as in the previous data, though in general, we obtain higher passages of the ions (lower retention of ions by the membrane). We closely reproduced the trend in how CCR influences ion passage. When CCR goes down, passage of cations increases, while at the same time, anion passage does not change as much. Temperature decreases ion passage for all ions, while the effect of pH is different for different ions. Thus, we can conclude that temperature, pH, and CCR affect ion passage of ions in the multi-ionic solution in different ways. We were able to come to this conclusion thanks to precise pH and temperature control (over prolonged periods) in this laboratory study. Future conceptual studies can be of aid to provide concrete answers to some of the trends observed in this paper. One option is to further develop ion transport models based on the data reported in this work.

■ ASSOCIATED CONTENT

Supporting Information

The Supporting Information is available free of charge at <https://pubs.acs.org/doi/10.1021/acsomega.1c02931>.

Comparison between old and new experimental methods, description of the methodology for the preparation of multi-ionic solution with sparsely soluble CaCO_3 , discussion on theoretical species in the tested multi-ionic solution and the influence of pH and temperature on them, and tables with experimental data (PDF)

AUTHOR INFORMATION

Corresponding Author

Edward M. Kimani – European Centre of Excellence for Sustainable Water Technology, Wetsus, 8911 MA Leeuwarden, The Netherlands; Membrane Science and Technology Cluster, University of Twente, 7522 NB Enschede, The Netherlands; orcid.org/0000-0002-8799-2481; Email: e.m.kimani@utwente.nl

Authors

Marko Pranić – European Centre of Excellence for Sustainable Water Technology, Wetsus, 8911 MA Leeuwarden, The Netherlands; Faculty of Chemical Engineering and Technology, University of Zagreb, 10000 Zagreb, Croatia

P. M. Biesheuvel – European Centre of Excellence for Sustainable Water Technology, Wetsus, 8911 MA Leeuwarden, The Netherlands; orcid.org/0000-0002-5468-559X

Slawomir Porada – European Centre of Excellence for Sustainable Water Technology, Wetsus, 8911 MA Leeuwarden, The Netherlands

Complete contact information is available at:
<https://pubs.acs.org/10.1021/acsomega.1c02931>

Notes

The authors declare no competing financial interest.

ACKNOWLEDGMENTS

This work was performed in the cooperation framework of Wetsus, European Centre of Excellence for Sustainable Water Technology (www.wetsus.eu). Wetsus is co-funded by the Dutch Ministry of Economic Affairs and Climate Policy, the Northern Netherlands Provinces, and the Province of Fryslân. The authors like to thank the participants of the research theme “Advanced Water Treatment” of Wetsus for fruitful discussions and financial support.

REFERENCES

- (1) United Nations General Assembly. Resolution A/RES/64/292. *The Human Right to Water and Sanitation*; United Nations, 2010.
- (2) Mekonnen, M. M.; Hoekstra, A. Y. Four billion people facing severe water scarcity. *Sci. Adv.* **2016**, *2*, No. e1500323.
- (3) Lopez-Gunn, E.; Ramón Llamas, M. Re-thinking water scarcity: Can science and technology solve the global water crisis? *Nat. Resour. Forum* **2008**, *32*, 228–238.
- (4) Fritzmann, C.; Löwenberg, J.; Wintgens, T.; Melin, T. State-of-the-art of reverse osmosis desalination. *Desalination* **2007**, *216*, 1–76.
- (5) Jones, E.; Qadir, M.; van Vliet, M. T. H.; Smakhtin, V.; Kang, S.-m. The state of desalination and brine production: A global outlook. *Sci. Total Environ.* **2019**, *657*, 1343–1356.
- (6) Adroit Market Research. *Water Desalination Market by Technology (Reverse Osmosis, Multi-Stage Flash Distillation, Hybrid Electrodialysis), Source (Seawater, Brackish Water) and Region, Global Forecasts 2018 to 2025*, 2020.
- (7) Verhuelsdonk, M.; Attenborough, T.; Lex, O.; Altmann, T. Design and optimization of seawater reverse osmosis desalination plants using special simulation software. *Desalination* **2010**, *250*, 729–733.
- (8) Qasim, M.; Badrelzaman, M.; Darwish, N. N.; Darwish, N. A.; Hilal, N. Reverse osmosis desalination: A state-of-the-art review. *Desalination* **2019**, *459*, 59–104.
- (9) Déon, S.; Escoda, A.; Fievet, P.; Dutournié, P.; Bourseau, P. How to use a multi-ionic transport model to fully predict rejection of mineral salts by nanofiltration membranes. *Chem. Eng. J.* **2012**, *189*–190, 24–31.
- (10) Stein, S.; Sivan, O.; Yechieli, Y.; Kasher, R. Redox condition of saline groundwater from coastal aquifers influences reverse osmosis desalination process. *Water Res.* **2021**, *188*, 116508.
- (11) Davidson, D. Amphoteric molecules, ions, and salts. *J. Chem. Educ.* **1955**, *32*, 550–559.
- (12) Nir, O.; Ophck, L.; Lahav, O. Acid-base dynamics in seawater reverse osmosis: Experimental evaluation of a reactive transport algorithm. *Environ. Sci.: Water Res. Technol.* **2016**, *2*, 107–116.
- (13) Kimani, E. M.; Kemperman, A. J. B.; Van Der Meer, W. G. J.; Biesheuvel, P. M. Multicomponent mass transport modeling of water desalination by reverse osmosis including ion pair formation. *J. Chem. Phys.* **2021**, *154*, 124501.
- (14) Tsuru, T.; Urairi, M.; Nakao, S.-i.; Kimura, S. Reverse osmosis of single and mixed electrolytes with charged membranes: Experiment and analysis. *J. Chem. Eng. Jpn.* **1991**, *24*, 518–524.
- (15) Biesheuvel, P. M.; Zhang, L.; Gasquet, P.; Blankert, B.; Elimelech, M.; van der Meer, W. G. J. Ion selectivity in brackish water desalination by reverse osmosis: Theory, measurements, and implications. *Environ. Sci. Technol. Lett.* **2020**, *7*, 42–47.
- (16) Tang, C. Y.; Chong, T. H.; Fane, A. G. Colloidal interactions and fouling of NF and RO membranes: A review. *Adv. Colloid Interface Sci.* **2011**, *164*, 126–143.
- (17) Bartels, C.; Franks, R.; Rybar, S.; Schierach, M.; Wilf, M. The effect of feed ionic strength on salt passage through reverse osmosis membranes. *Desalination* **2005**, *184*, 185–195.
- (18) Bhattacharjee, T.; Jiang, H.; Behdad, N. A fluidic colorimetric sensor design for water hardness detection. *IEEE Sens. J.* **2015**, *15*, 819–826.
- (19) van der Aa, M. Classification of mineral water types and comparison with drinking water standards. *Environ. Geol.* **2003**, *44*, 554–563.
- (20) The European Parliament and the Council of the European Union. Directive (EU) 2020/2184 on the quality of water intended for human consumption. *Off. J. Eur. Communities* **2020**, *63*, 1–62.
- (21) Mosley, L. M.; Daly, R.; Palmer, D.; Yeates, P.; Dallimore, C.; Biswas, T.; Simpson, S. L. Predictive modelling of pH and dissolved metal concentrations and speciation following mixing of acid drainage with river water. *Appl. Geochem.* **2015**, *59*, 1–10.
- (22) Xu, Y.; Hu, H.; Liu, J.; Luo, J.; Qian, G.; Wang, A. pH dependent phosphorus release from waste activated sludge: Contributions of phosphorus speciation. *Chem. Eng. J.* **2015**, *267*, 260–265.
- (23) Weiss, R. F. Carbon dioxide in water and seawater: The solubility of a non-ideal gas. *Mar. Chem.* **1974**, *2*, 203–215.
- (24) Dickson, A. G. The carbon dioxide system in seawater: Equilibrium chemistry and measurements. In *Guide to Best Practices for Ocean Acidification Research and Data Reporting*; Riebesell, U., Fabry, V. J., Hansson, L., Gattuso, J. P., Eds.; Publications Office of the European Union: Luxembourg, 2010; Vol. 260, pp 17–52.
- (25) Zhan, N.; Huang, Y.; Rao, Z.; Zhao, X.-L. Fast detection of carbonate and bicarbonate in groundwater and lake water by coupled ion selective electrode. *Chin. J. Anal. Chem.* **2016**, *44*, 355–360.
- (26) Legrand, L.; Schaetzle, O.; De Kler, R. C. F.; Hamelers, H. V. M. Solvent-free CO₂ capture using membrane capacitive deionization. *Environ. Sci. Technol.* **2018**, *52*, 9478–9485.
- (27) Torres, C. I.; Lee, H.-S.; Rittmann, B. E. Carbonate species as OH⁻ carriers for decreasing the pH gradient between cathode and anode in biological fuel cells. *Environ. Sci. Technol.* **2008**, *42*, 8773–8777.
- (28) Kim, M.-J.; Nriagu, J.; Haack, S. Carbonate ions and arsenic dissolution by groundwater. *Environ. Sci. Technol.* **2000**, *34*, 3094–3100.
- (29) Parbs, A.; Ebert, M.; Dahmke, A. Long-term effects of dissolved carbonate species on the degradation of trichloroethylene by zerovalent iron. *Environ. Sci. Technol.* **2007**, *41*, 291–296.
- (30) Agrawal, A.; Ferguson, W. J.; Gardner, B. O.; Christ, J. A.; Bandstra, J. Z.; Tratnyek, P. G. Effects of carbonate species on the kinetics of dechlorination of 1,1,1-trichloroethane by zero-valent iron. *Environ. Sci. Technol.* **2002**, *36*, 4326–4333.

- (31) Lado Ribeiro, A. R.; Moreira, N. F. F.; Li Puma, G.; Silva, A. M. T. Impact of water matrix on the removal of micropollutants by advanced oxidation technologies. *Chem. Eng. J.* **2019**, *363*, 155–173.
- (32) MacAdam, J.; Parsons, S. A. Calcium carbonate scale formation and control. *Rev. Environ. Sci. Biotechnol.* **2004**, *3*, 159–169.
- (33) Hall, M. S.; Starov, V. M.; Lloyd, D. R. Reverse osmosis of multicomponent electrolyte solutions Part I. Theoretical development. *J. Membr. Sci.* **1997**, *128*, 23–37.
- (34) Tu, K. L.; Chivas, A. R.; Nghiem, L. D. Effects of membrane fouling and scaling on boron rejection by nanofiltration and reverse osmosis membranes. *Desalination* **2011**, *279*, 269–277.
- (35) Riedel, T. Temperature-associated changes in groundwater quality. *J. Hydrol.* **2019**, *572*, 206–212.
- (36) Jin, X.; Jawor, A.; Kim, S.; Hoek, E. M. V. Effects of feed water temperature on separation performance and organic fouling of brackish water RO membranes. *Desalination* **2009**, *239*, 346–359.
- (37) Sharma, R. R.; Chellam, S. Temperature effects on the morphology of porous thin film composite nanofiltration membranes. *Environ. Sci. Technol.* **2005**, *39*, 5022–5030.
- (38) Goosen, M. F. A.; Sablani, S. S.; Al-Maskari, S. S.; Al-Belushi, R. H.; Wilf, M. Effect of feed temperature on permeate flux and mass transfer coefficient in spiral-wound reverse osmosis systems. *Desalination* **2002**, *144*, 367–372.
- (39) Biesheuvel, P. M.; Dykstra, J. E. *Physics of Electrochemical Processes*; ISBN: 9789090332581, 2020; pp 283–288.
- (40) Coronell, O.; Mi, B.; Mariñas, B. J.; Cahill, D. G. Modeling the effect of charge density in the active layers of reverse osmosis and nanofiltration membranes on the rejection of arsenic(III) and potassium iodide. *Environ. Sci. Technol.* **2013**, *47*, 420–428.
- (41) Hoang, T.; Stevens, G.; Kentish, S. The effect of feed pH on the performance of a reverse osmosis membrane. *Desalination* **2010**, *261*, 99–103.
- (42) Van Wagner, E. M.; Sagle, A. C.; Sharma, M. M.; Freeman, B. D. Effect of crossflow testing conditions, including feed pH and continuous feed filtration, on commercial reverse osmosis membrane performance. *J. Membr. Sci.* **2009**, *345*, 97–109.
- (43) Donose, B. C.; Premavally, A. V.; Pype, M.-L.; Doederer, K. Selective laser assisted impairment of reverse osmosis membranes. *MethodsX* **2020**, *7*, 100830.